

Texture-based Computer-Assisted Diagnosis for fiberoptic Images

Christian Münzenmayer, Christian Winter, Stephan Rupp, Andreas Kage, Thomas Wittenberg

Abstract—Flexible endoscopes based on fiber bundles are still widely used despite the recent success of so-called tip-chip endoscopes. This is partly due to the costs and that for extremely thin diameters (below 3 mm) there are still only fiberscopes available. Due to the inevitable artifacts caused by the transition from the fiber bundles to the sensor chip, image and texture analysis algorithms are severely handicapped. Therefore, texture-based computer-assisted diagnosis (CAD) systems could not be used in such domains without image pre-processing.

We describe a CAD system approach that includes an image filtering algorithm to remove the fiber image artifacts first and then applies conventional color texture algorithms that have been applied to other endoscopic disciplines in the past. The concept is evaluated on an image database with artificially rendered fiber artifacts so that ground truth information is available.

I. INTRODUCTION

Flexible endoscopy was for a long time inseparably connected to the notion of fiberoptic image transmission which is based on a bundle of glass or quartz fibers. Usually, glass fibers exhibit a regular structure of the fiber bundles whereas cheaper quartz fibers have irregular shapes and orientations (see figure 1). In the recent years so-called tip-chip endoscopes which bear the sensor chip on the distal end of the endoscope conquered the market and replaced classical fiberscopes in areas such as gastroscopy or bronchoscopy. Nevertheless, due to the costs they are still widely used in private practice as well as for extremely narrow body openings. E.g. in the ear-nose-throat (ENT) discipline the pharynx is examined via fiberoptic nose-pharyngoscopes that are typically equipped with 10,000 to 30,000 fibers and an outer diameter of about 3 mm. The incidence of carcinoma of the pharynx increased steadily over the last 20 years and amounts to 4 out of 100,000 per year in Germany today. Mouth and oropharyngeal cancer account for 1.7% of diagnosed cancers in the UK. Another application is the so-called cholangioscopy which is the inspection of the bile ducts by a fiberoptic endoscope. This so-called babycholangioscope is inserted through the working channel of a conventional duodenoscope into the bile ducts. Bile duct cancer (cholangiocarcinoma) has an incidence of about 1-2 cases per 100,000 population per year in the US and UK. For Japan and Israel the incidence is much higher with 5.5 to 7.3 cases per 100,000 people a year.

C. Münzenmayer, C. Winter, S. Rupp, A. Kage, T. Wittenberg are with the Fraunhofer Institute for Integrated Circuits IIS, 91058 Erlangen, Germany
christian.muenzenmayer@iis.fraunhofer.de

This work was partially funded by the Collaborative Research Center 603 by the German Research Foundation (DFG).

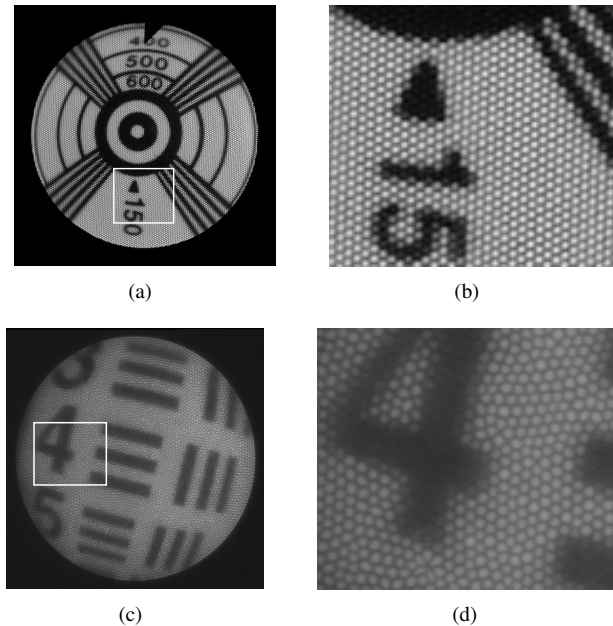


Fig. 1. Typical view through a (a) glass fiberscope and (c) a quartz fiberscope onto a test chart. The enlarged sections depict the (b) homogeneous honeycomb structure from the glass fiber transmission and (d) the inhomogeneous and irregular structure of the quartz fibers.

Therefore, slim fiberscopes are still of major importance in diagnosis and treatment of cancer. On the other hand, there has been done a lot of work with respect to computer-assisted diagnosis (CAD) in the recent years. Mainly started in the area of mammography and chest radiography but in the last 10 years more and more work has been done for endoscopic applications as well. These are applications such as the automatic detection of polyps within colonoscopic video images as published in [1], [2], [3], the classification of leukoplakia on images of the vocal folds from rigid endoscopes as described by Ilgner et al. [4] or the computer-assisted diagnosis of Barrett's esophagus from gastroscopic images [5].

All of these methods rely more or less on the extraction of textural features such as co-occurrence matrices [6], sum- and difference-histograms (SDH) [7], wavelet features [8], local binary patterns [9], or Gabor filters [10]. However, to our knowledge no one ever tried to apply such algorithms to fiberoptic images which are very difficult to analyse due to the unavoidable artifacts imposed by the construction. These are, a 'honey-comb' like structure overlaid over the image due to the fibers and the cladding which appears black in the image as well as color artifacts introduced by the imperfect fitting of the fiber centers onto the color-filter array of the

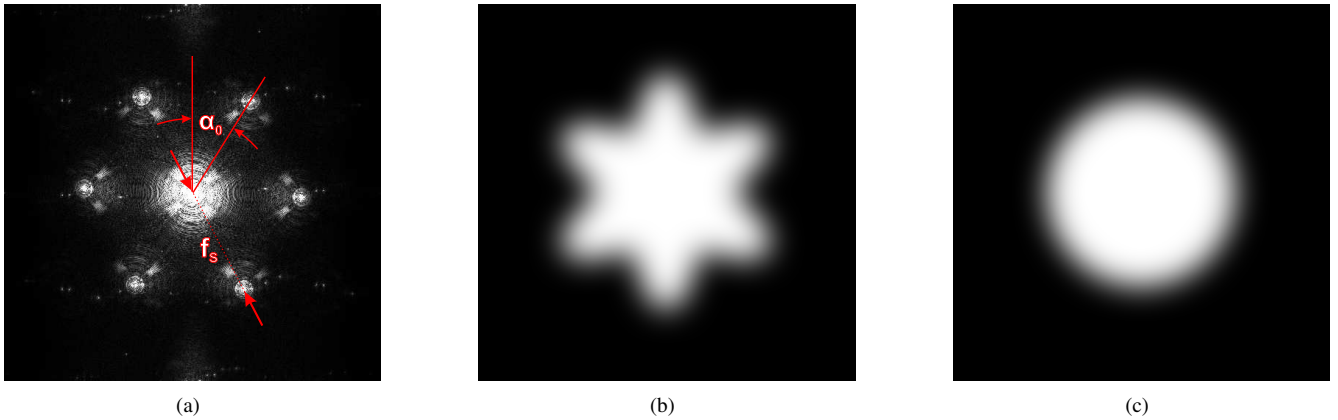


Fig. 2. Typical spectrum of fiberoptic image with clustered frequency peaks (a). Rotation variant star-shaped mask (b) with angle α_0 and structure frequency f_s versus rotation invariant circular mask (c) to damp or eliminate irrelevant frequency parts.

commonly used Bayer pattern one-chip cameras.

In this paper we describe and evaluate a concept for a texture-based CAD system suitable for fiberoptic image material. Therefore, the images are processed by a method to remove the honey-comb structure from the images before texture features are extracted (section II). To corroborate the proof-of-concept we simulated the fiber artifacts on a large, annotated image database of cases from Barrett's esophagus and show how different texture features behave before and after processing of the images in comparison to the results on the original image database (section III). These results are discussed in section IV. We conclude in V.

II. TEXTURE-ANALYSIS ON FIBERSCOPIC IMAGES

A. Fiberoptic image filtering

To free fiberoptic images from their characteristic 'honey-comb' structure, we use an automatic filter approach with adapted filter mask generation. Winter et al. [11] describe the background and application of algorithms to generate optimal spectral filter masks for enhancement of fiberoptic images. The Nyquist-Shannon Sampling Theorem is taken into account to obtain optimal parameters for filter mask calculation. Due to its flexibility and almost equal quantitative filter results we use rotation invariant masks (see figure 2(c)) instead of the sophisticated starshaped rotation variant masks (see figure 2(b)). The filtering is performed in the frequency domain by damping and eliminating non-relevant parts of the spectrum (see figure 2(a)). Applying the approach to all three image planes the cited method is extended to color image processing. Due to simplification we accept some non-visible approximations with respect to color aberration and spectral cross talking between fibers. The approach works automatically and independently of scale and resolution of the fiberscopes' image conductor as well as type and resolution of the image sensor. The result is a structure free image that contains a maximum of relevant scene information.

B. Feature extraction

Chen et al. [12] derive a set of statistical geometrical features (SGF) from a decomposition of a gray-level image into a stack of binary images. Therefore, a series of thresholds is used. Afterwards connected regions are determined in each binary image by using a connected neighborhood and for every binary image, the number of connected regions and their average weighted irregularity are determined. With statistics of these values over the binary stack 16 gray level features are computed. By boolean operations the binary images computed from the different color channels of an image can be combined to form a new set color texture features as described in [13]. For the purpose of this work the SGF in the inter-plane version by use of an XOR operation which proved to be the most powerful of these variants will be used as described in the next section.

The sum- and difference-histograms introduced by Unser et al. [7] are a computationally efficient approximation of the well-known co-occurrence matrix features. This algorithm is based on the computation of a histogram of the gray-level differences and sums of neighbored pixels which are characterized by 15 scalar features. In the color domain these features can be computed for each plane (intra-plane mode) or by sums and differences of pixels from different planes (inter-plane) as shown in [14]. Both of these variants will be used for the evaluation of the fiberoptic image filtering.

Gabor filters have received a great attention in the fields of texture segmentation, edge detection and other imaging tasks. Wanderley et al. [10] published an illumination-invariant version of color Gabor filters which compute features appropriate to the current scale. Together with this algorithm we used four different feature sets for the experimental evaluation.

III. EXPERIMENTS AND RESULTS

In order to substantiate the proof-of-concept of the fiberoptic CAD system an image database with annotated image regions is necessary to evaluate the classification accuracy. To evaluate the effects of the fiberoptic filtering algorithm

TABLE I
CLASSIFICATION ACCURACY OF DIFFERENT TEXTURAL FEATURE
EXTRACTORS ON THE ORIGINAL, THE ARTIFICIALLY FIBERED, AND THE
FILTERED IMAGES WITH LEAVE-ONE-OUT SAMPLING.

Features	Accuracy [%]		
	Original	Fibered	Filtered
SGF XOR	76	65	76
SDH inter	67	65	65
SDH intra	78	66	76
Gabor	80	71	80

ground truth data is needed. Typically that would not be available with real fiberoscopic images. Therefore, we choose the approach to use an image database without fiber artifacts, simulate the fiberoscopic structures, filter the images and compare the results for all three sets. Here, we use an image database with zoom-endoscopic images from a video-gastroscope (Olympus EVIS Exera 160). Within this database there are 350 images from the esophagus that have been captured after acid instillation (for contrast enhancement). On these images 451 regions of interest (ROI) have been marked and classified by a gastroenterologist based on the histologic findings. Included are 129 images of gastric mucosa, 164 images of Barrett's esophagus and 158 images showing squamous epithelium.

To simulate the effect of fiberoscopic image acquisition a method previously presented by Rupp et al. [15], [16] has been used. This method uses a reference image from a fiberoscopic system to capture the fiber structure by locating the fiber centers first. These centers are tessellated by the Delaunay triangulation and from the corresponding Voronoi net the cladding of the fibers is approximated. The accumulated intensity of a fiber is distributed to the overlapping pixels according to a two dimensional Gaussian distribution positioned at the fiber center. To these so-called 'fibered' images the reconstruction algorithm described in section II-A was applied before features were extracted. A sample image before and after the *fiberizing* process as well as the filtered result is shown in figure 3.

In an attempt to adapt to the scale of the lesions the images were filtered by a binomial filter and sub-sampled by a factor of four in each dimension before the SDH and SGF features are calculated. For the Gabor filters this step is not necessary as these features are computed on several levels anyway. For every ROI annotated by a clinical expert we have extracted a vector of numerical features as described above. To evaluate the classification accuracy leave-one-out sampling strategy was used with a nearest-neighbor classifier after statistical normalization of features.

Table I shows the classification accuracy for three different families of feature extractors that have been described in section II-B.

IV. DISCUSSION

The inter-plane statistical geometrical features (SGF XOR) drop from 76% by 11% from the original images to the

artificially fibered images. With the exception of the intra-plane sum- and difference histograms there is a similar collapse for all features. However, the intra-plane SDH features have already a quite low classification accuracy which is diminished only insignificantly by the artificial fiberizing. Therefore, the filtering does not really show a great effect here. In all cases the accuracy on the filtered images reaches the same or a by 2% reduced classification accuracy. Hence, the relevant texture information could be reconstructed by the filtering algorithm. Of course, it has to be noted that this depends on the Nyquist criterion, i.e. that structures that are smaller than two fiber diameters cannot be resolved adequately.

We also want to point out that despite the binomial filtering and subsampling which might resolve the issue of fiber artifacts at first glance, the classification results deteriorate. Therefore, an appropriate filtering algorithm such as the one we propose, is inevitable for processing such image material. Finally, it can be noted that these results have been achieved on three fundamentally different algorithms as have been distinguished in the important work of Randen and Husoy [17]. The sum- and difference histograms are a representative of statistical texture features, Gabor filters are one of the most frequently used spectral texture measures and the statistical geometrical features are a hybrid form of geometrical primitives and statistical features. Therefore, with some confidence it can be assumed that these results could generalize to other feature families in a similar way.

V. CONCLUSION

We presented the concept of a texture-based CAD system for fiberoscopic images which is based on an optimized image filtering algorithm to remove the honey-comb structure and color texture features for the classification of image regions. The results from simulated fiberoscopic images showed that the filtering allowed almost perfect reconstruction, so that the fiber artifacts influenced the classification accuracy only insignificantly or not at all. This result is insofar of significant importance as to our knowledge up to now no one ever tried to apply texture analysis to fiberoscopic image material or even build a computer-assisted diagnosis system in that way.

Due to the available ground truth this comparison could be made very efficiently. Now that these results are available, the next step that has to follow is to build representative image databases with annotated regions from real fiberoscopic applications, e.g. in the ENT domain. Based on this data an evaluation under real-world conditions should be focused on.

REFERENCES

- [1] S. M. Krishnan and P. M. Goh, "Quantitative parameterization of colonoscopic images by applying fuzzy technique," in *Proc's 19th IEEE Int. Conf. Engineering in Medicine and Biology Society (EMBS)*, 1997, pp. 1121 – 1123.
- [2] P. Wang, S. M. Krishnan, C. Kugean, and M. P. Tjoa, "Classification of Endoscopic Images Based on Texture and Neural Network," in *Proc. of the 23rd Annual EMBS Int. Conf., Oct. 25.-28., Istanbul, Turkey*, 2001, pp. 3691–3695.

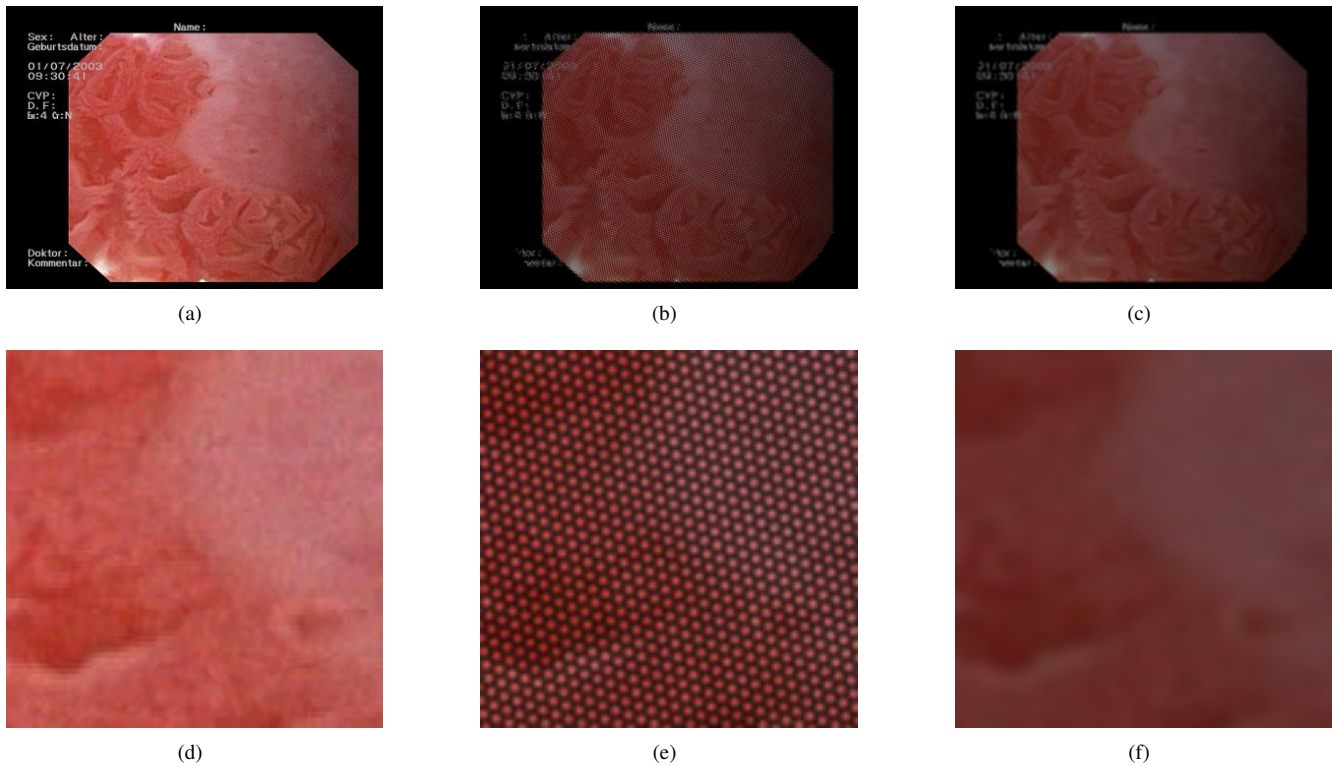


Fig. 3. Example image from the Barrett's esophagus database: (a) original image, (b) fibered image, (c) filtered image. (d-f) detail images.

- [3] S. A. Karkanis, D. K. Iakovidis, D. E. Maroulis, D. A. Karras, and M. Tzivras, "Computer-aided tumor detection in endoscopic video using color wavelet features," *IEEE Trans. on Informatics Technology in Biomedicine*, vol. 7, no. 3, pp. 141 – 151, 2003.
- [4] J. H. Illgner, C. Palm, A. Schütz, K. Spitzer, M. Westhofen, and T. M. Lehmann, "Colour texture analysis for quantitative laryngoscopy," *Acta Oto-Laryngologica*, vol. 123, pp. 730–734, 2003.
- [5] A. Kage, C. Münzenmayer, and T. Wittenberg, "A knowledge-based system for the computer assisted diagnosis of endoscopic images," in *Bildverarbeitung für die Medizin 2008*, ser. Reihe Informatik Aktuell, T. Tolxdorff, J. Braun, T. Deserno, H. Handels, A. Horsch, and H.-P. Meinzer, Eds., Workshop. 6. - 8.4.2008 in Berlin. Springer, Verlag Heidelberg, 2008, pp. 272 – 276.
- [6] R. Haralick, K. Shanmugam, and I. Dinstein, "Textural features for image classification," *IEEE Trans. Syst. Man Cyb.*, vol. SMC-3, no. 6, pp. 610–621, November 1973.
- [7] M. Unser, "Sum and difference histograms for texture analysis," *IEEE Transactions on Pattern Analysis and Machine Intelligence*, vol. 8, no. 1, pp. 118–125, 1986.
- [8] G. V. de Wouwer, P. Scheunders, S. Livens, and D. V. Dyck, "Wavelet correlation signatures for color texture characterization," *Pat. Rec.*, vol. 32, no. 3, pp. 443–451, 1999. [Online]. Available: citeseer.nj.nec.com/vandewouwer99wavelet.html
- [9] T. Ojala, M. Pietikäinen, and T. Mäenpää, "Multiresolution gray-scale and rotation invariant texture classification with local binary patterns," *IEEE Trans. Pattern Anal. Mach. Intell.*, vol. 24, no. 7, pp. 971–987, 2002.
- [10] J. F. C. Wanderley and M. H. Fisher, "Multiscale color invariants based on the human visual system," *IEEE Trans. Image Process.*, vol. 10, no. 11, pp. 1630–1638, November 2001.
- [11] C. Winter, S. Rupp, M. Elter, C. Münzenmayer, H. Gerhäuser, and T. Wittenberg, "Automatic adaptive enhancement for images obtained with fiberscopic endoscopes," *IEEE Trans. Biomed. Eng.*, vol. 53, no. 10, pp. 2053–2046, October 2006.
- [12] Y. Q. Chen, M. S. Nixon, and D. W. Thomas, "Statistical geometrical features for texture classification," *Pat. Rec.*, vol. 28, no. 4, pp. 537–552, September 1995.
- [13] C. Münzenmayer, "Color texture analysis in medical applications," Ph.D. dissertation, Universität Koblenz-Landau, Der Andere Verlag, Tönnig, Lübeck und Marburg, 2006.
- [14] C. Münzenmayer, H. Volk, C. Küblbeck, K. Spinnler, and T. Wittenberg, "Multispectral texture analysis using interplane sum- and difference-histograms," in *Pattern Recognition - Proceedings of the 24th DAGM Symposium Zurich, Switzerland*, L. V. Gool, Ed. Berlin: Springer, 2002, pp. 25–31.
- [15] S. Rupp, C. Steenkamp, and C. Winter, "Imaging Models for the Evaluation of Fiber-Optic Image Processing Algorithms," in *International Conference on Image Processing, Computer Vision, and Pattern Recognition (IPCV'09)*, July 2009.
- [16] S. Rupp, C. Winter, and M. Elter, "Improving the accuracy of feature extraction for flexible endoscope calibration by spatial super resolution," in *Proceedings of the 29th Annual International Conference of the IEEE Engineering in Medicine and Biology Society*. IOP Publishing, Bristol, August 2007, pp. 6565–71.
- [17] T. Randen and J. H. Husoy, "Filtering for texture classification: A comparative study," *IEEE Trans. Pattern Anal. Mach. Intell.*, vol. 21, no. 4, pp. 291–310, April 1999.